7.8 LENGTH SCALES OF REMOTELY SENSED VEGETATION, SURFACE RADIOMETRIC TEMPERATURE, AND DERIVED SURFACE ENERGY FLUXES

Nathaniel A. Brunsell* and Robert R. Gillies
Utah State University, Logan, UT

1. Introduction

The interaction between length scales in vegetation and temperature with the partitioning of surface energy fluxes is examined. These interactions are important for assessing the feasibility of incorporating satellite estimates of controlling biophysical variables into regional meteorological
and climatological models.

Horizontal length scales are computed via wavelet multiresolution analysis for remotely sensed fractional vegetation (Gillies and Carlson, 1995) and radiometric temperature at two different resolutions collected during the Southern Great Plains 1997 (SGP97) Hydrology Experiment. The first resolution is airborne Thermal Infrared Multispectral Scanner (TIMS) temperature and Thematic Mapper Simulator (TMS) fractional vegetation (Fr) at 12 meter pixel resolution. The second resolution is from the Advanced Very High Resolution Radiometer (AVHRR) with approximately 1000 meter pixel resolution.

The remotely sensed data are coupled to a Soil-Vegetation-Atmosphere-Transfer (SVAT) model using the "Triangle Method" of Gillies et al. (1997) to estimate pixel scale latent and sensible heat fluxes. The modeled fluxes are compared to surface fluxes and an aggregation scheme is proposed for computing large scale radiometric temperature from high resolution data. Wavelet cospectra are used to determine the interaction between remotely sensed input and modeled surface fluxes.

2. Length scales of remotely-sensed data and derived fluxes

The spectra are computed from a wavelet multiresolution analysis. This analysis is conducted at dyadic scales and the spectra is calculated from the wavelet variance as (Kumar and Foufoula-Georgiou, 1997):

$$W_\lambda = \sum_x D(\lambda, x)^2 \quad (1)$$

where $D(\lambda,x)$ are the wavelet coefficients at scale λ and position x, and W_λ is the wavelet variance at scale λ. The length scale is then the scale where the wavelet variance reaches a maximum.

**Corresponding author address*: Nathaniel Brunsell, Dept. of Plants, Soils and Biometeorology, Logan, UT 84322-4820; email: brunsell@cc.usu.edu

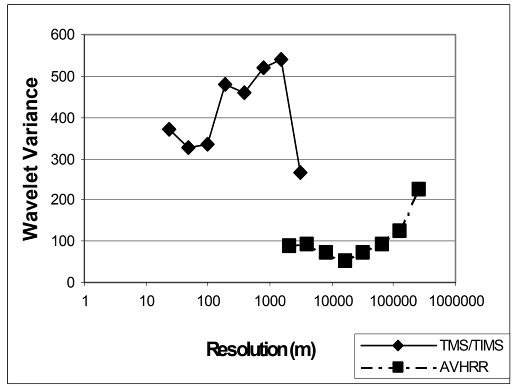

Fig 1. Wavelet spectra for TMS/TIMS and AVHRR evaporation.

Length scales of Fr and temperature for the airborne data are approximately 800 meters (corresponding well to the average field size). The TIMS temperature shows an additional peak at the 24 m scale. The AVHRR data shows a remarkably different pattern. The Fr and temperature fields are both dominated by large-scale variability on the order of 256,000 m. However, the cospectra between AVHRR temperature and Fr exhibits an additional peak on the order of 2000 m.

The TMS/TIMS derived evaporation shows a peak on the order of 1500 m (Figure 1), and the sensible heat shows a peak on the order of 24 m. The wavelet cospectra between the vegetation and the TMS/TIMS derived fluxes (Figure 2) all show peaks on the order of 800 meters, however the 24 m scale dominates the wavelet spectra. The cospectra between AVHRR fractional vegetation and the derived fluxes show predominantly smaller scale variability, with evaporation exhibiting an additional peak on the order of 125000 m.

The TIMS temperature and evaporation

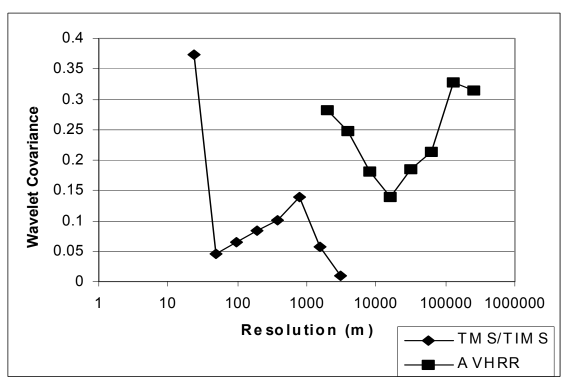

Fig 2. Wavelet cospectra for TMS/TIMS and AVHRR evaporation and Fr.

cospectra show the 800 m peak with the additional 24 peak dominating (Figure 3). The AVHRR cospectra between the derived evaporation and the temperature exhibit a peak at the 256000 m scale, and very little small scale variance. The sensible heat flux shows the large scale variance, but has the additional peak at the 2000 m scale.

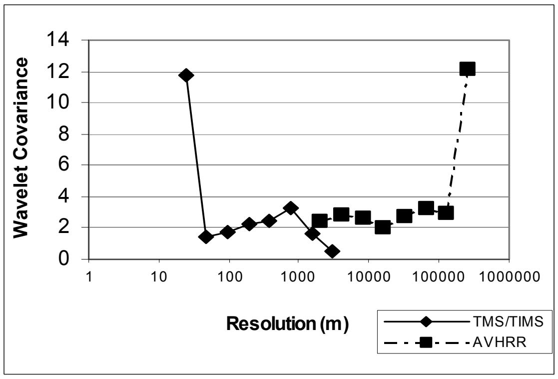

Fig 3. Wavelet cospectra for TMS/TIMS and AVHRR evaporation and temperature.

3. Comparison with surface measurements and aggregation

The airborne derived fluxes agree fairly well with the four eddy-covariance stations located within the El Reno study area. Pixelwise comparisons are on the order of 15 % RMSE for both sensible and latent heat fluxes. However, AVHRR derived fluxes have 77% and 50 % errors for sensible and latent heat fluxes.

Aggregation of the dominant variables (e.g. radiometric temperature and fractional vegetation) was then assessed. Fractional vegetation can not be averaged linearly, but the Normalized Difference Vegetation Index (NDVI) can be and the Fr can be computed from the areal average of the NDVI. In order to aggregate the radiometric temperature, the following formula was used:

$$\overline{T} = \left(\frac{\varepsilon_v Fr T_v^{\ 4} + \varepsilon_s (1 - Fr) T_s^{\ 4}}{Fr \cdot \varepsilon_v + (1 - Fr) \cdot \varepsilon_s} \right)^{1/4} \qquad (2)$$

where $\overline{T}$ is the pixel radiometric temperature, and the denominator on the right hand side is the effective pixel emissivity (Brunsell and Gillies, 2001), ε_s is the soil emissivity and ε_s represents the vegetation emissivity. When AVHRR fluxes are compared to TMS/TIMS aggregated fluxes yield good agreement with RMSE of 35 % for sensible heat and 11% for latent heat. This shows remarkable agreement given the poor agreement between AVHRR and surface measurements, but relatively good agreement between TMS/TIMS fluxes and the surface.

4. Conclusions

The airborne data are dominated by the presence of a 800 m length scale in both the fractional vegetation and the radiometric temperature fields. The temperature data also exhibit a length scale on the order of 24 m. The cospectra between these data and the derived energy fluxes show small scale behavior on the order of 24 m. This indicates that the fluxes are responding primarily to small scale differences in temperature (due to the fact that no peak is observed at 24 m in the Fr data), rather than changes in the fractional vegetation.

In the case of the AVHRR, the large scale variability dominates. The cospectra between Fr and temperature exhibits a small scale (2000 m) peak not observed in either spectra individually. This small scale activity is observed in the evaporation Fr cospectra. This is due to the radiative balance of the surface. With the AVHRR data, the initial pixel size is too coarse to observe local (field to field) variability in Fr that dominated over the temperature variability in the high resolution airborne data. At coarser pixel resolution (2000 m), the Fr spatial variability dominates over the importance in the temperature data, resulting in the peak in the evaporation at 2000 m. However, at even larger scales, neither Fr nor temperature dominates and the resultant fluxes have large contributions from both fields.

5. References

Brunsell, N.A. and R. R. Gillies, 2001: An algorithm for incorporating surface emissivity into a thermal atmospheric correction. Submitted to *Photogramatic Engineering and Remote Sensing.*

Gillies, R. R. and T.N. Carlson, 1995: Thermal remote sensing of surface soil water content with partial vegetation cover for incorporation into climate models. *Journal of Applied Meteorology*, **34**(4), 745-756.

Gillies, R., T. Carlson, J. Cui, W. Kustas, and K. Humes, 1997: A verification of the 'triangle' method for obtaining surface soil water content and energy fluxes from remote measurements of the normalized difference vegetation index (NDVI) and surface radiant temperature. *International Journal of Remote Sensing*, **18**(15), 3145-3166.

Kumar, P. and Foufoula-Georgiou, E., 1997: Wavelet analysis for geophysical applications. *Reviews of Geophysics*, **35**, 385-412.